

# Neurochemical measurements in the zebrafish brain

Lauren Jones<sup>1</sup>, James McCutcheon<sup>1</sup>, Andrew Young<sup>1</sup>, William Norton<sup>1\*</sup>

<sup>1</sup>Neuroscience, Psychology and Behaviour, University of Leicester, United Kingdom

Submitted to Journal: Frontiers in Behavioral Neuroscience

Article type: Original Research Article

*Manuscript ID:* 148886

Received on: 22 Apr 2015

Revised on: 18 Aug 2015

Frontiers website link: www.frontiersin.org

1	Neurochemical measurements in the zebrafish brain
2	
3	Lauren J Jones, James E McCutcheon, Andrew MJ Young <sup>*</sup> and William HJ Norton <sup>*</sup>
4	
5 6	Department of Neuroscience, Psychology and Behaviour, University of Leicester, Leicester, LE1 7RH, UK
7	*Correspondence:
8	Dr Andrew Young
9	Department of Neuroscience, Psychology and Behaviour
10	University of Leicester,
11	University Rd,
12	Leicester, LE1 7RH, UK
13	amjy1@le.ac.uk
14	
15	and
16	
17	Dr William Norton
18	Department of Neuroscience, Psychology and Behaviour
19	University of Leicester,
20	University Rd,
21	Leicester, LE1 7RH, UK
22	whjn1@le.ac.uk
23	
24	
25	
26	
27	7330 words and 10 figures
28	
29	

#### 30 Abstract

31 The zebrafish is an ideal model organism for behavioural genetics and neuroscience. The high conservation of genes and neurotransmitter pathways between zebrafish and other vertebrates permits 32 the translation of research between species. Zebrafish behaviour can be studied at both larval and 33 adult stages and recent research has begun to establish zebrafish models for human disease. Fast scan 34 35 cyclic voltammetry (FSCV) is an electrochemical technique that permits the detection of neurotransmitter release and reuptake. In this study we have used in vitro FSCV to measure the 36 release of analytes in the adult zebrafish telencephalon. We compare different stimulation methods 37 and present a characterisation of neurochemical changes in the wild-type zebrafish brain. This study 38 represents the first FSCV recordings in zebrafish, thus paving the way for neurochemical analysis of 39 40 the fish brain.

41

42 <u>Keywords:</u> Zebrafish, Fast scan cyclic voltammetry, Adult brain, Dopamine, 5-HT, Histamine, pH,
 43 Neurochemistry

#### 44 Introduction

45 A central goal of neuroscience is to understand how the brain processes stimuli in order to tailor an 46 appropriate behavioural response. Initially, each behaviour was thought to be driven by a dedicated neural circuit in the brain (Zupanc and Lamprecht, 2000). However, recent research suggests that 47 48 discrete behaviours can be produced by the interaction of diffuse neural networks with overlapping 49 functions (Bargmann, 2012). Thus, dramatically different behaviours can be driven by the same 50 neurons acting in parallel circuits. Rather than being hard-wired entities, neural circuits exhibit 51 plasticity due to short-term neuromodulatory activity and longer-term structural reorganisation at the 52 synaptic level (Zupanc and Lamprecht, 2000; Bargmann, 2012). Therefore, a combination of 53 approaches combining information from a range of scientific disciplines is needed to identify the 54 network components that drive behaviour.

55 The zebrafish is a powerful model organism for developmental biology and neuroscience. Zebrafish 56 are also an ideal species to investigate the neural circuits that drive behaviour since their relative 57 transparency until larval stages permits the visualisation and manipulation of neurons within the intact 58 brain (Feierstein et al.; Fetcho and Liu, 1998; Arrenberg and Driever, 2013; Bonan and Norton, 2015). 59 Neural circuits can be mapped using calcium imaging, bioluminescence or electrophysiology to 60 monitor neural activity in freely behaving fish (Higashijima et al., 2003; Naumann et al., 2010). Techniques such as genetic ablation or optogenetics can then be used to functionally connect circuits 61 to behaviour (Nagel et al., 2003;Curado et al., 2007;Zhang et al., 2007;Del Bene and Wyart, 2012). 62 An alternative approach, based upon forward genetics, is to identify mutant lines that exhibit 63 64 interesting behavioural phenotypes. The expression profile of the mutated loci can be used as a 65 starting point to examine the alterations to brain structure and function that underpin aberrant 66 behaviour (Webb et al., 2009;Norton et al., 2011;Ziv et al., 2013).

67 Previous studies have used quantitative PCR, immunohistochemistry and electrophysiology to 68 investigate the function of the zebrafish brain. In our laboratory we complement these approaches by 69 using fast-scan cyclic voltammetry (FSCV) to quantify the release- and reuptake of neurotransmitters at the synapse on a sub-second time-scale (Stamford, 1990;Heien et al., 2004). A voltage waveform is 70 71 applied to a carbon fibre microelectrode causing oxidation and reduction of electroactive compounds at the surface of the electrode (Stamford, 1990; John and Jones, 2007a). These oxidation and reduction 72 73 reactions lead to changes in electrical current which are proportional to the concentration of the 74 compound being measured. This data can be visualised as a colour plot where current is encoded 75 using a false colour scheme and plotted against both applied electrical potential  $(E_{app})$  and time (Heien 76 et al., 2004). Typically, in vitro neurotransmitter release is evoked by using either electrical 77 stimulation or bath application of a high concentration of potassium. Different analytes, including 78 many neurotransmitters, can be identified on the basis of their voltammograms (a plot of applied 79 voltage against current) using attributes such as the position, shape and relative amplitude of the 80 oxidation and reduction peaks (Stamford, 1990;Heien et al., 2004). Further specificity can be achieved by placing the recording electrode into brain areas containing a single neurotransmitter or by applying 81 82 specific drugs that modify neurotransmitter reuptake (Dankoski and Wightman, 2013). Finally, if 83 stimulation evokes the release of several analytes, the overlapping voltammograms can be separated 84 by principal component analysis (Heien et al., 2004).

In this study we present a method for FSCV recordings in sagittal slices of the adult zebrafish brain
and characterise the release of analytes in the telencephalon. This research provides a basis for
examination of zebrafish mutants that display intriguing behavioural phenotypes by uncovering
alterations to the dynamics of neurotransmitter release in the brain.

89

#### 90 Materials and Methods

91 Fish Stocks

All experiments were performed on adults of the AB/AB wild-type strain. Standard fish keeping
protocols and conditions were followed (Westerfield, 1995). Fish were anaesthetised in MS333 and
culled by decapitation (a Schedule 1 procedure under the Animals (Scientific Procedures) Act 1986
Amendment Regulations 2012). All protocols are covered by appropriate personal licences: PIL
60/13671 (WHJN) and PIL I98F58CD7 (LJJ).

#### 98 FSCV equipment

97

99 The setup for FSCV was custom built and consists of a tissue bath, stimulating electrode, recording 100 and reference electrodes connected to a computer and amplifier (Fig. 1A). Carbon fibre 101 microelectrodes (tip size 7x120 μm) were used as recording electrodes and an Ag/AgCl electrode as a 102 reference. The recording and reference electrodes were connected to a potentiostat and headstage 103 circuit (ChemClamp, Dagan Instruments, USA) and a computer running TarHeel (Chapel Hill, 104 University of North Carolina) voltammetry software. The waveform (Fig. 1A) was applied at 10 Hz.

#### 105 <u>Electrode manufacture</u>

106 Glass capillary electrodes were used for all our FSCV experiments. Electrodes were manufactured as described in Fortin et al., 2015. A single carbon fibre was aspirated into a borosilicate glass capillary 107 (World Precision Instruments, 100 mm length, 1/0.58 mm OD/ID). The glass was pulled to a fine tip 108 109 using a vertical needle puller (PE-21, Narishige) and the exposed carbon fibre was cut to a length of 100 µm using a scalpel. A wire coated in silver conductive paint (Coating Silver Print II, GC 110 111 Electronics) was inserted into the capillary, secured with a gold pin (Newark) and heat shrinkwrapped to the capillary (FP-301, 3M). In each case, electrodes were tested to ensure a suitable 112 background (non-Faradaic) current profile by applying the voltage waveform (see below) at 60 Hz. If 113 the current signal was adequate the electrode was cycled at 60 Hz for a minimum of 15 minutes to 114 reduce background drift. 115

#### 116 <u>Voltage input waveforms</u>

117 The voltage input waveform was scanned at a rate of 400 V/second in the following pattern:  $0 \text{ V} \rightarrow$ 118 +1.2 V  $\rightarrow$  -0.6 V  $\rightarrow$  0 V (John and Jones, 2007a). With this waveform, dopamine oxidises at ~+0.6 V 119 and shows one reduction peak at ~-0.2 V; 5-HT oxidises at ~+0.6 V and shows two reduction peaks at 120 ~0 V and ~-0.5 V; and histamine shows two reduction peaks on the forward scans of the waveform at 121 ~+0.25 V and ~-0.4 V and an oxidation peak on the reverse scan at ~+1.05 V.

#### 122 Flow cell experiments

Flow cell experiments were performed in a custom-built Y-shaped chamber (University of Illinois at 123 124 Chicago Biology Workshop (Sinkala et al., 2012)). The cell permits a carbon-fibre electrode to be exposed to known concentrations of neurotransmitter solutions. All analytes were dissolved in 125 artificial fish cerebrospinal fluid (aCSF) and delivered by gravity perfusion at a rate of 1 ml per 126 minute. aCSF (pH 7.4) contained (in mM) 131 NaCl, 2 KCL, 1.25 KH<sub>2</sub>PO<sub>4</sub>, 2 MgSO<sub>4</sub>, 20 NaHCO<sub>3</sub>, 127 128 2.5 CaCl, and 10 glucose (Vargas et al., 2011). For some experiments, we prepared aCSF containing 20 mM 4-(2-hydroxyethyl)-1-piperazineethanesulphonic acid (HEPES) adjusted to pH 7.4. The 129 voltage waveform was applied to electrodes at 60 Hz for 15 minutes prior to the start of each 130 131 experiment to precondition the electrode (Fortin et al., 2015). Known concentrations of dopamine, 132 histamine, 5-HT, and pH-adjusted aCSF were perfused for 5 seconds and changes in current were 133 recorded.

#### 134 Preparation of tissue for FSCV

135 Following decapitation, the brain was manually dissected from the skull in a Petri dish containing ice-

136 cold aCSF. Brains were sliced sagittally and transferred to a tube containing additional ice-cold aCSF.

137 Sections were mounted in an organ bath and perfused with oxygenated aCSF (constantly bubbled with 138 95%  $O_2$  and 5%  $CO_2$  and warmed to 32°C by a Peltier heater) at a rate of 1.5 ml per minute. Tissue

sections were allowed to equilibrate in warmed aCSF for 10-15 minutes before recording began. The

140 flow rate was regulated by a gravity flow system containing an intravenous dial flow-regulator (World

- 141 Precision Instruments) and waste aCSF was aspirated using a Dymax 5 suction pump (Charles Austen
- pumps and RS Components). A micromanipulator (R.C-2R adjustable clamp, Narishige) was used to
- 143 insert the electrodes into the telencephalon at a depth of approximately 150  $\mu$ m (Fig. 1B).

#### 144 <u>Stimulation of neurotransmitter release</u>

145 Neurotransmitter release was evoked by either bath application of a high concentration of potassium or electrical stimulation. Potassium-evoked release was performed by perfusing tissue with high K<sup>+</sup> 146 (100 mM, replacing an equimolar amount of NaCl) aCSF for 1 minute once a stable 30-second 147 148 baseline recording had been obtained. Electrically-evoked release was performed with a bipolar stimulating electrode placed close to the carbon fibre recording electrode within the dorsal 149 150 telencephalon. Current pulses were generated by the acquisition software and applied via a stimulus isolator (Iso-Flex; AMP Instruments). The tissue was allowed to recover for a minimum of either 5 151 152 minutes (electrical stimulation) or 30 minutes (for high  $K^+$  stimulation) between stimulations. In some 153 experiments we added drugs targeting neurotransmitter systems to the aCSF: 10 µM GBR 12909 (selective DA reuptake inhibitor; Sigma Aldrich D052); or 10 µM cocaine hydrochloride (DA, NA 154 and 5-HT reuptake inhibitor; Sigma Aldrich C5776). GBR 12909 was first dissolved in DMSO with 155 gentle warming before being directly added to the aCSF. Cocaine was made into a stock solution in 156 157 water before being added to aCSF. Drugs were not perfused onto tissue until at least 3 stable baseline 158 recordings had been obtained.

#### 159 <u>Fast-scan cyclic voltammetry procedure</u>

Voltage waveforms were applied to electrodes using TarHeel software and the resulting changes to current were recorded and analysed. Carbon fibre microelectrodes generate a characteristic background signal that can be subtracted to yield the Faradaic current caused by oxidation and reduction of compounds (Fig. 1C (Baur et al., 1988;John and Jones, 2007a)). Neurotransmitters were identified upon the basis of their cyclic voltammograms (noting the position and height of oxidation and reduction peaks) and colour plots permitted the visualisation of release dynamics over time.

#### 166 <u>Statistical analyses</u>

The percentage of variance in experimental data (voltammograms recorded in the telencephalon) 167 accounted for by template data (voltammograms generated in a flow cell) was assessed using the CV 168 match programme in TarHeel (Robinson et al., 2003). Analyses were only performed on experimental 169 data obtained using the same electrode as that used to collect template data. We reported the values as 170  $r^2$ , which was deemed to be significant when exceeding a threshold of  $r^2 = 0.75$  as described in Heien 171 et al., 2003. Principal component analysis was performed in TarHeel (Heien et al., 2004;Heien et al., 172 2005;Keithley and Wightman, 2011). An in vitro training set composed of cyclic voltammograms for 173 dopamine, 5-HT, histamine and both acidic and basic pH shifts and combinations of these four factors 174 175 were used for the final analysis (Heien et al., 2004; Heien et al., 2005). At least 5 voltammograms for each species (neurotransmitter / pH change) or combination were included. Training sets were 176 177 deemed to fit the data appropriately if the maximum value shown on the Q plot did not exceed the 178 threshold Qa value (686681). Current vs. time data recorded following application of neurotransmitter 179 reuptake inhibitors to the tissue were extracted from TarHeel software and imported into Clampfit 10.2 (part of pCLAMP 10.2 software package; Molecular Devices). Baseline correction was applied 180 181 to all recordings to account for increasing / decreasing baselines and electrode drift thus ensuring a stable flat baseline for analysis. Clampfit was also used for peak analysis, providing values for peak 182 183 amplitude and multiple time parameters reflective of reuptake. This included half width, (the time taken for the peak to reach- and return to half peak amplitude), T half (time taken to decay to half 184 185 peak amplitude from peak), tau decay (a time constant representing decay of current), and peak area (nA\*s) all of which have been deemed appropriate measures of neurotransmitter reuptake (Yorgason 186 187 et al., 2011). Statistical analyses were conducted using GraphPad Prism 6 for Windows. One-way repeated measures ANOVA tests were performed for all measures, with time as the repeated measures 188 189 variable. Control values were obtained by averaging values from 3 control stimulations prior to drug

perfusion. When statistical significance was indicated (p < 0.05), post-hoc analyses were conducted using Dunnett's multiple comparisons test, comparing each time-point to control and adjusting pvalues accordingly. Non-parametric Friedman tests were used when data were not normally distributed. When statistical significance was indicated, post-hoc analyses were conducted using Dunn's multiple comparisons test adjusting p values accordingly.

195

#### 196 <u>Results</u>

#### 197 <u>Characterisation of neurotransmitter profiles in a flow cell</u>

198 As a first step towards characterising analyte release in zebrafish we collected template FSCV data for 199 dopamine, 5-HT and histamine, neurotransmitter systems that send extensive projections to the 200 telencephalon. We used a flow cell (Sinkala et al., 2012), a microfluidic device that permits electrodes to be exposed to standard neurotransmitter solutions, to collect representative colour plots and cyclic 201 voltammograms. We exposed carbon fibre electrodes to a known concentration of each 202 neurotransmitter or pH shift (using the voltage waveform shown in Fig. 3B). Application of 1 µM 203 dopamine produced an increase in current at ~+0.6 V and a reduction peak at ~-0.25 V (Fig. 2A and 204 205 2B). A 0.5  $\mu$ M 5-HT solution also produced an increase in current ~+0.6 V but reduction peaks 206 occurred at ~0 V and ~-0.5 V (Fig. 2C and 2D). Application of 40 µM histamine produced a very different response, with an increase in current on the reverse scan at  $\sim+1.0$  V and two reduction peaks 207 208 on the forward scan at ~+0.25 V and ~-0.4 V (Fig. 2E and Fig. 2F). We also investigated the effect of altering pH on the oxidation potentials of voltammograms. An acidic change of -0.25 pH units (i.e. 209 210 pH 7.15) produced an oxidation peak at ~+0.5 V and reduction peaks at both ~+1.1V and ~-0.3 V (Fig. 2G and 2H). An acidic change of -1.0 pH units (i.e. pH 6.4) produced a similar voltammogram 211 with a sharp oxidation peak at ~+0.5 V and reduction peaks at both ~+1.1 V and ~-0.3 V (Fig. 2I and 212 213 2J). A basic pH change of +1.0 units (i.e. pH 8.4) produced a large oxidation peak on the reverse scan at  $\sim+1.1$  V and reduction peaks on the forward scans at  $\sim+0.4$  V and  $\sim-0.5$  V, similar to the 214 neurotransmitter histamine (Fig. 2K and 2L). Together, these experiments demonstrate the 215 characteristic shapes of cyclic voltammograms that are produced by exposing electrodes to 216 neurotransmitter solutions and changes in pH. 217

#### 218 Fast scan cyclic voltammetry in the adult zebrafish brain

We next investigated whether fast scan cyclic voltammetry (FSCV) could be used to measure the 219 release of analytes in sagittal sections of the adult zebrafish brain. The zebrafish dorsal telencephalon 220 receives extensive 5-HT-positive projections from the raphe- and pretectal nuclei (Lillesaar et al., 221 222 2009). We therefore applied a voltage waveform optimised for measurements of 5-HT (John and Jones, 2007a) and depolarised neurons and terminals with aCSF containing a high concentration of K<sup>+</sup> 223 (100 mM K<sup>+</sup>; hereafter high K<sup>+</sup> aCSF). Bath application of high K<sup>+</sup> aCSF led to changes in current at 224 225 several points in the voltage waveform. A cyclic voltammogram extracted at ~10 seconds after stimulation displays characteristics that could reflect the oxidation of dopamine and/or 5-HT, 226 227 including a prominent peak in current on the forward scan at ~+0.6 V (Fig. 3E). A rapid increase in 228 oxidative current is observed at the point in the waveform that corresponds to the peak of this signal 229  $(\sim+0.6 \text{ V}; \text{ Fig. 3C})$ . However, this current vs. time plot also exhibits a striking dip in current which is 230 most likely due to the decrease in current at around  $\sim+0.2$  V masking the oxidation peak at  $\sim+0.6$  V.

The cyclic voltammogram extracted 30 seconds after application of high K<sup>+</sup> aCSF displays a different 231 232 set of characteristics that are suggestive of an additional compound being oxidised on the reverse scan of the waveform (Fig. 3F). These features include a dip in current at ~+0.6 V, a large increase in 233 234 current at around ~+1.0 V and two decreases in current at ~+0.2 V and ~-0.4 V suggesting that reduction occurs on the forward scan of the waveform (Fig 3D and 3F). Examination of the current vs. 235 236 time plot at +1.0 V shows a large increase in current that returns towards baseline upon washout of the high K<sup>+</sup> aCSF (Fig 3D). The cyclic voltammogram of the second analyte exhibited characteristics of 237 238 the voltammogram for the neurotransmitter histamine (Fig. 2F) which has distinct characteristics

239 including a reduction peak on the forward scan and an oxidation peak on the reverse scan (in contrast to the oxidation and reduction profile of dopamine (Fig. 2B) and 5-HT (Fig. 2D) (Pihel et al., 240 1995;Hashemi et al., 2011;Chang et al., 2012). Interestingly, both current vs. time plots reveal a long 241 time-course of release with analytes failing to return fully to pre-stimulation baseline levels. We next 242 compared FSCV data obtained from multiple independent experiments (n=12 sagittal sections from 8 243 fish for data extracted at  $\sim 10$  seconds, and n=12 sagittal sections from 8 fish for data extracted at  $\sim 30$ 244 seconds). The shape of the voltammograms that we obtained was highly reproducible, both within-245 246 and across experiments (Fig. 3G and 3H). Furthermore, average voltammograms compiled from these 247 experiments looked similar to representative recordings in the telencephalon, with oxidation- and 248 reduction peaks occurring at the same potentials (compare Fig. 3I to 3E and 3J to 3F). This suggests that we can compare FSCV data across different animals or mutant lines. 249

#### 250 <u>Electrically-evoked neurotransmitter release in the zebrafish telencephalon</u>

251 Bath application of high  $K^+$  aCSF produced a current vs. time plot with a prolonged release profile that did not return to pre-stimulation baseline levels. In order to clarify whether this was an artefact 252 caused by electrode drift during the long time necessary for complete washout to occur, we used 253 254 electrical stimulation to evoke the release of analytes (Fig. 4A). Electrical stimulation of local terminals using optimal parameters (20 pulses with a pulse width of 4 ms, 60 Hz, 500  $\mu$ A) resulted in 255 256 an increase in current on the forward part of the waveform (Fig. 4C and 4F) that rapidly returned to 257 baseline (n=8 stimulations from a single sagittal section in Fig. 4C and 4B). It also produced a cyclic voltammogram with a shape similar to that obtained using high K<sup>+</sup> aCSF suggesting that both types of 258 stimulation evoke the release of a similar mixture of analytes (Fig. 4B and 4E). We tested this 259 possibility using the CV match algorithm in TarHeel. Comparison of an example electrical 260 stimulation with an example K<sup>+</sup> stimulation gave an  $r^2$  value of 0.876, indicating that both types of 261 stimulation evoke similar neurochemical changes in the tissue. However, the oxidation peak at  $\sim+0.6$ 262 V and reduction peak at  $\sim -0.2$  V were much more prominent when using electrical stimulation than in 263 voltammograms obtained using high K<sup>+</sup> aCSF. The lowest intensity stimulation that we could use to 264 trigger analyte release in the telencephalon was 20 pulsed with a pulse width of 4 ms, 60 Hz, 300 µA. 265 This produced a voltammogram with an oxidation peak at  $\sim +0.6$  V and a smaller reduction peak at 266 ~0.2 V (Fig. 4H and 4I). In contrast to this, high intensity stimulation (1 mA, 60 Hz, 60 pulses, pulse 267 width 4 ms) produced a cyclic voltammogram with a similar shape to that extracted  $\sim 30$  s after K<sup>+</sup> 268 stimulation (Fig. 4J and 4K) with a small oxidation peak occurring on the reverse scan at  $\sim 1.1$  V and a 269 large reduction peak at ~-0.4 V). Furthermore, the change in current ~+0.6 V showed a large decrease 270 similar to the dip in current observed following  $K^+$  stimulation (Fig. 4L). The prolonged time-course 271 of alterations in current suggested that an artefact such as a change in pH had occurred. This indicates 272 that stimulation parameters are an important consideration when attempting to obtain reproducible 273 measurements of neurotransmitter release that are not masked by pH shifts or electrode drift. 274

#### 275 Analysis of the effects of pH changes on current following stimulation of the telencephalon

276 We investigated whether a shift in pH could be contributing to the changes in the current that we measured by adding HEPES buffer to the aCSF. Stimulation using high K<sup>+</sup> HEPES-buffered aCSF 277 278 altered the release profile of analytes occurring at the oxidation and reduction potentials for both dopamine and histamine. The large dip normally present at ~10 seconds after application of high  $K^+$ 279 280 aCSF was reduced (compare Fig. 5A and 5C with 5B and 5D). Furthermore, addition of HEPES caused the current to return to baseline following stimulation (Fig. 5D) suggesting a less prominent 281 shift in background signal. The resulting voltammogram, taken ~10 seconds after stimulation, (Fig. 282 5E) no longer showed a large reduction in signal at around +0.2 V which seemed to mask the 283 284 oxidation peak at +0.6 V in previous experiments (compare to Fig. 3A and 3C). A second cyclic voltammogram taken ~30 seconds after stimulation showed a small increase in current observed at 285 ~+0.7 V (Fig. 5F). 286

#### 287 <u>Combinations of neurotransmitter solutions in the flow cell</u>

288 The colour- and voltage plots that we obtained from recordings in the zebrafish telencephalon 289 appeared to be influenced by the release of more than one analyte. We applied combinations of dopamine, 5-HT and histamine and pH changes to the electrode in the flow cell and measured changes 290 291 in current. A combination of 1  $\mu$ M dopamine and 40  $\mu$ M histamine produced a cyclic voltammogram with a small oxidation peak at  $\sim+0.6$  V, a larger oxidation peak at around +1.0 V and three reduction 292 293 peaks at ~+0.25 V, ~-0.2 V and ~-0.4 V (Fig. 6A). A combination of 2 µM dopamine and 20 µM 294 histamine produced a very large oxidation peak at  $\sim+0.6$  V, a second oxidation peak on the reverse scan at ~+1.0 V and reduction peaks at ~+0.2 V, ~-0.2 V and ~-0.4 V (Fig. 6B). Likewise, combining 295 5-HT and histamine produced a voltammogram with a similar oxidation profile but different reduction 296 profile. A mixture of 0.25 µM 5-HT and 40 µM histamine led to oxidation peaks at ~+0.6 V and 297 ~+1.0 V and reduction peaks at ~+0.3 V, ~0 V and ~-0.4 V (Fig. 6C). We also examined the current 298 299 changes produced by mixing all three neurotransmitters. A combination of 0.25  $\mu$ M 5-HT, 1  $\mu$ M dopamine and 20  $\mu$ M histamine produced a current plot with oxidation peaks at ~+0.6 V and ~+1.0 V 300 and four reduction peaks at ~+0.2 V, ~0 V, ~-0.2 V and ~-0.4 V (Fig. 6D). Together, these data 301 302 indicate that it should be possible to separate signals composed of these three neurotransmitters, since 303 each individual peak is neither inflated nor altered by the presence of a second compound, apart from the overlapping oxidation peak at ~+0.6 V for dopamine and 5-HT. However, 5-HT can still be 304 identified by its unique reduction peaks, permitting the visual dissociation of these two transmitters. 305 We explored the possibility that pH changes could be influencing the signals that we recorded in the 306 307 telencephalon by altering the pH of dopamine, histamine and 5-HT mixtures in a flow cell. A combination of -0.5 pH units, 1 µM dopamine and 40 µM histamine (Fig. 6E) produced a cyclic 308 voltammogram similar to the voltammogram obtained ~10 seconds after high K<sup>+</sup> aCSF stimulation 309 310 (Fig. 2D). Altering the pH of histamine alone (80 uM histamine and -0.25 pH units; Fig. 6F) provided a good in-vitro representation of the voltammogram for the second analyte obtained with high K<sup>+</sup> 311 312 HEPES-buffered aCSF (Fig. 6E,F). Despite not being completely identical, it showed changes in current at ~+0.2 V, ~+1.0 V, and ~-0.4 V. A basic change in pH (+1.0 units) coupled to 1 µM 313 dopamine and 40  $\mu$ M histamine produced a voltammogram with a broad reduction peak around +0.4 314 315 V (Fig. 6G) but no large reduction peak at ~-0.4 V (Fig. 5E and 5F) suggesting that the pH change was not likely to be basic. Furthermore, addition of 5-HT to the flow cell mixture also produced a 316 voltammogram with a very different shape (1 µM 5-HT, 80 µM histamine and -0.5 pH units) 317 318 suggesting that 5-HT was unlikely to have contributed to the analytes measured in the telencephalon 319 (Fig. 6H).

#### 320 <u>CV match analysis of in vitro stimulation data</u>

In order to compare the similarity of experimental recordings in tissue to template flow cell data we 321 used the CV match function in TarHeel. We calculated  $r^2$  values between experimental cyclic 322 voltammograms from the telencephalon obtained using optimal stimulation parameters and multiple 323 template cyclic voltammograms (Robinson and Wightman, 2007). Comparison of voltammograms 324 325 produced by electrical stimulation (4 experiments from 2 sagittal sections taken from 2 fish) to a mixture of 2  $\mu$ M dopamine, 80  $\mu$ M histamine and an acidic pH shift of -0.25 units produced  $r^2$  values 326 that exceeded the accepted threshold of 0.75 in 3 out of 4 stimulations analysed (for example, Fig. 7A 327 and 7C,  $r^2 = 0.846$ ; 7A and 7E,  $r^2 = 0.833$ ; for further values see Table 1). In one case, a template of 4 328  $\mu$ M dopamine, 160  $\mu$ M histamine and an acidic pH shift of -0.25 units produced the highest  $r^2$  value 329 of 0.878 (see table 1). High  $K^+$  aCSF stimulation of the telencephalon produced a voltammogram at 330  $\sim 10$  s following stimulation, which we also compared to multiple template cyclic voltammograms (2) 331 experiments from 2 fish) that were significantly similar to a combination of 2 µM dopamine and 20 332  $\mu$ M histamine (Fig. 7B and 7D,  $r^2 = 0.857$ ; for further values see Table 1). However it was not 333 possible to produce a template voltammogram in the flow cell that gave a significant match to a 334 voltammogram extracted at ~30 s following high  $K^+$  aCSF stimulation. In summary, the analytes 335 336 released by electrical stimulation of the zebrafish forebrain are significantly similar to a combination of dopamine, histamine and an acidic pH change of -0.25 units, whereas the analytes released -10337

seconds after high  $K^+$  stimulation are indicated to be more similar to a combination of dopamine and histamine.

#### 340 Principal component analysis of electrical stimulation data

341 We examined our data using principal component analysis to provide an estimate of actual neurotransmitter concentration in the brain and to determine the relative contribution of each 342 343 neurotransmitter to the changes in current that we measured (Heien et al., 2005;Keithley and Wightman, 2011). We constructed training sets of voltammograms that included responses to both 344 single neurotransmitters and mixtures of neurotransmitters in the flow cell. Full details of these 345 346 training sets are provided in Table 1. We used data from electrical stimulation experiments (Fig. 8A) for this analysis because recordings using high K<sup>+</sup> aCSF did not fit the statistical model well, perhaps 347 348 due to the prolonged time-course of the changes that can cause the baseline to drift. We obtained the best fit for our electrical stimulation data (i.e. the lowest residual values) when using a training set that 349 350 included dopamine, 5-HT, histamine and both acidic- and basic pH shifts. The resulting concentration 351 vs. time plots suggest that dopamine (Fig. 8C), 5-HT (Fig. 8D) and histamine (Fig. 8E) are all likely to be present following electrical stimulation. Importantly, the resulting Qt plot did not pass the 352 threshold of 686681 at any point (Fig. 8G) suggesting that our training set fits the in vitro data well. 353 354 The increase of dopamine is ~100 nM, 5-HT ~8.0 nM and the increase of histamine is ~8.0  $\mu$ M. In addition, it appears that there is also an acidic pH shift of ~0.05 units (Fig. 8F). To confirm that our 355 356 PCA was accurate in its representation of type- and concentration- of analytes, we examined a combination of 0.25 µM 5HT, 1 µM dopamine, 40 µM histamine and an acidic pH shift of +1.0 unit 357 obtained in the flow cell. This provided a highly accurate prediction of the concentration of each 358 359 species (Fig. 8H), suggesting that the training set was indeed appropriate for the main analysis.

#### 360 Pharmacological inhibition of dopamine reuptake

The identity of analytes released during FSCV can be further confirmed by pharmacological 361 validation (Dankoski and Wightman, 2013). The results of the CV match and PCA analyses suggest 362 that dopamine is likely to be a major contributor to the changes in current that we measured. We 363 further investigated this prediction by manipulating dopamine pharmacologically. We treated sagittal 364 slices of the adult zebrafish brain with either cocaine, a non-selective monoamine reuptake inhibitor 365 366 that has been shown to increase dopamine reuptake within the rodent nucleus accumbens, caudate putamen and substantia nigra (Jones et al., 1995a;Jones et al., 1995b;Davidson et al., 2000;John and 367 Jones, 2007a; John and Jones, 2007b; España et al., 2008; Yorgason et al., 2011) or the selective long-368 acting dopamine reuptake inhibitor GBR 12909 (España et al., 2008;Esposti et al., 2013). Treatment 369 with 10  $\mu$ M cocaine produced an increase in current at ~+0.6 V that appeared to be prolonged (Fig. 370 371 9B-D) compared to controls (Fig. 9A). Current vs. time plots showed peaks that become broader over time (Fig. 9E-H) indicating a slowing down of reuptake kinetics. Comparison of cyclic 372 373 voltammograms from these experiments further demonstrated that oxidation- and reduction peaks 374 became more prominent at ~+0.65 V and ~-0.25 V respectively (Fig. 9I-L) following cocaine application, with a shape that was more similar to the dopamine voltammogram obtained in the flow 375 376 cell (Fig. 2B). Current vs. time plots further illustrated this, as peaks became broader over time (Fig. 377 9I-L) indicating a slowing down of reuptake kinetics. Moreover, there was a slight increase in the 378 amplitude of peaks (Fig. 9M,N), suggesting that cocaine may also affect dopamine release in the 379 zebrafish telencephalon. We used one-way repeated measures ANOVA tests followed by Dunnett's 380 multiple comparisons tests with *p*-value adjustment to compare the average value of three control stimulations with 4 time-points following cocaine perfusion (n=6 fish in each case). Non parametric 381 382 tests were used when the data were not normally distributed. There was a significant effect of cocaine on peak height (nA; F(4,20) = 4.91, p < 0.01). Post hoc Dunnett's tests revealed that peak height was 383 significantly larger than control at 10 minutes (p < 0.005), 20 minutes (p < 0.005) and 30 minutes (p < 0.005) 384 0.05) after cocaine perfusion, but not after 40 minutes (p > 0.05). Cocaine also had a significant effect 385 386 0.01), 20 minutes (p < 0.0001), 30 minutes (p < 0.0001) and 40 minutes (p < 0.0001) after perfusion. 387 There was also a significant effect on T Half (s; F(4,20) = 23.23, p < 0.0001). T Half was significantly 388 increased at 10 minutes (p = 0.005), 20 minutes, (p < 0.0001), 30 minutes (p < 0.0001) and 40 389

390 minutes (p < 0.0001). Cocaine also significantly influenced peak area (nA\*s; F(4,20) = 19.17, p < 10000.0001). Dunnett's tests revealed peak area was significantly larger 10 minutes, (p < 0.005), 20 391 minutes (p < 0.0001), 30 minutes (p < 0.0001) and 40 minutes (p < 0.0001) following cocaine 392 perfusion. Tau decay (s) was also significantly altered ( $\chi^2(5) = 18.53$ , p = 0.001 Friedman test). Post 393 hoc tests showed that tau decay was significantly larger 20 minutes (p = 0.001), 30 minutes (p < 0.05) 394 and 40 minutes (p < 0.005) following cocaine application. Treatment with 10  $\mu$ M of the more 395 selective dopamine reuptake inhibitor GBR 12909 led to an increase in the amplitude and time course 396 397 of current at ~+0.6 V following electrical stimulation (Fig. 10 A-D). The related current vs. time plots 398 show that peaks become larger and somewhat broader over time indicating an increase in release and 399 possibly a slowing of reuptake kinetics as well (Fig. 10E-H). Comparison of cyclic voltammograms from these experiments provided further evidence for an increase in the amplitude of release, as the 400 401 peak around the oxidation potential for dopamine (~+0.65 V) became considerably larger (Fig. 10I-L). The effects of 10 µM GBR 12909 application were analysed using non parametric tests to account 402 403 for significant deviation from normality. Friedman tests followed by post hoc Dunn's multiple comparisons with p-value adjustment were used to compare the average value of three control 404 405 stimulations with 4 time-points post GBR 12909 perfusion (n=6 fish in each case). GBR 12909 had a significant effect on peak height (nA;  $\gamma^2(5) = 16.93$ , p < 0.005). Peak height was significantly 406 407 increased after 30 minutes, (p < 0.05) and 40 minutes (p < 0.0001) drug application. GBR 12909 did not significantly alter half width (s; p = 0.0504), however there was a significant effect on T half (s; 408 409  $\chi^2(5) = 10.4$ , p < 0.05). Dunn's tests revealed that T half was significantly increased after 20 minutes, (p < 0.05), 30 minutes (p < 0.05) and 40 minutes (p < 0.05). There was also a significant effect of 410 GBR 12909 on peak area (nA\*s;  $\chi^2(5) = 14.67$ , p < 0.01). Peak area was significant increased after 20 411 412 minutes, (p < 0.05), 30 minutes, (p < 0.05), and 40 minutes, (p < 0.005) GBR 12909 perfusion. GBR 12909 did not significantly alter tau decay (p > 0.05). Taken together, the combination of statistical 413 414 analysis and pharmacological studies demonstrates that stimulation of the telencephalon evokes the release of dopamine, with possible release of histamine and a concomitant acidic change in pH as 415 416 well.

417

#### 418 Discussion

419 In this study we have established a protocol to record the release of analytes in the zebrafish 420 telencephalon by FSCV. We evoked neurotransmitter release by either bath application of high  $K^+$ aCSF or by electrical stimulation of local terminals. Neurotransmitters were detected and identified 421 422 upon the basis of their oxidation and reduction profiles at the surface of a carbon fibre electrode. Using this method we obtained voltammograms that are significantly similar to the simultaneous 423 measurement of dopamine and histamine coupled to a change in pH. We have also provided 424 425 pharmacological validation that we have measured the release of dopamine. To the best of our knowledge, this study represents the first FSCV recordings in zebrafish, thus paving the way for 426 neurochemical analysis of the fish brain. 427

#### 428 <u>Comparison of slice preparation and method of stimulation</u>

429 There are several advantages to using an in vitro slice preparation rather than recording from whole brains. Firstly, we were able to accurately place electrodes in a specific area, something that would be 430 difficult to achieve in intact brains in the absence of a stereotaxic atlas. Our setup also gave us fine-431 432 control of environmental parameters (including temperature and pH) and obviated the need to use an anaesthetic which could potentially alter the dynamics of neurotransmitter release (John and Jones, 433 2007a). We also compared stimulation of neurotransmitter release by either perfusion of high  $K^+$ 434 435 aCSF or electrical stimulation. The results that we obtained with both methods were comparable once 436 we had identified the best parameters for electrical stimulation (20 pulses with a pulse width of 4 ms, 60 Hz, 500 µA). The data that we obtained using low intensity stimulation was not very reproducible, 437 and the oxidation peak was less prominent than in experiments using optimal parameters. In contrast 438 439 to this, high intensity electrical- or K<sup>+</sup> aCSF stimulation triggered a prolonged release profile that did 440 not return to baseline. Electrical stimulation is ideal for examining local neurotransmitter release and

441 could in theory be used to map neural circuits in the brain. However, we will have severed a large
442 number of axon tracts when sectioning the brain meaning that the action of some endogenous control
443 mechanisms (such inhibitory neurotransmitters) may have been disrupted (Dankoski and Wightman,

444 2013). The results from our slice preparation thus need to be interpreted with caution.

#### 445 Identity of neurotransmitters recorded in the telencephalon

446 A major challenge of fast scan cyclic voltammetry is to characterise the analytes that are released following stimulation. Wightman and colleagues have suggested five criteria that can be used to 447 identify endogenously released substances (Dankoski and Wightman, 2013): good correlation 448 449 between voltammograms obtained during an experiment and standard data (e.g. when exposing electrodes to neurotransmitter solutions in a flow cell); independent verification of the presence of the 450 neurotransmitter; precise anatomical positioning of the electrode in the region of interest; correct 451 physiological release properties for the transmitter being measured; and pharmacological validation of 452 each compound (Dankoski and Wightman, 2013). We have taken these criteria into account in this 453 454 study. We compared our FSCV recordings in brain slices to template cyclic voltammograms generated in a flow cell using the CV match software (Fig. 2, 6 and 7). 5-HT, dopamine and histamine 455 have already been shown to be present in the zebrafish forebrain by high pressure liquid 456 457 chromatography and radioactive immunoassay (Norton et al., 2011;Buske and Gerlai, 2012). Furthermore, the position of our recording electrode was chosen based upon studies of the projection 458 patterns of dopamine, 5-HT- and histamine neurons (Kaslin and Panula, 2001;Lillesaar et al., 2009). 459 The voltammograms that we obtained from recordings in the telencephalon appear to represent a 460 combination of more than one neurotransmitter. We do not appear to be measuring 5-HT since the 461 462 voltammograms in Fig. 3D do not show the characteristic reduction peak at 0 V (see Fig. 3D). Our 463 telencephalic recordings are most similar to an acidic (pH 6.95) solution of  $\sim 2 \mu M$  dopamine and 80 µM histamine recorded in the flow cell (Fig. 7). We further validated this result by using the selective 464 dopamine reuptake inhibitor GBR 12909 (Esposti et al., 2013). Application of GBR 12909 led to a 465 significant alteration in peak amplitude, area and reuptake. We could not use the Michaelis-Menten 466 467 kinetics to analyse this data, since the rate of dopamine reuptake in zebrafish (i.e. the rate of DOPAC formation in tissue slices) has not been calculated (Near et al., 1988) and it is unlikely that the 468 469 stimulated release saturated reuptake, a prerequisite for Michaelis-Menten modelling. However, peak amplitude, area and reuptake parameters have already been used to examine FSCV data following 470 pharmacological manipulation (Yorgason et al., 2011) demonstrating the validity of this approach. 471

#### 472 <u>Characteristics of neurotransmitter release in the zebrafish telencephalon</u>

The initial current vs. time plots that we recorded following high  $K^+$  aCSF stimulation of the 473 474 telencephalon had two striking characteristics: a long release profile that lasted approximately 5 minutes (Fig. 3C, 3E); and the presence of a second analyte that did not return to baseline (Fig. 3F). 475 476 Increasing the intensity of electrical stimulation also led to a longer time-course of release (Fig. 4L). 477 This result was surprising, since measurements of neurotransmitter release in the rodent brain typically only last for a few seconds (Hashemi et al., 2011). However, it could also indicate that a pH 478 479 change has altered the background signal and thus inflated our measurements of current (Jones et al., 480 1994; Takmakov et al., 2010). Acidifying or alkalising pH shifts can occur in conjunction with neurotransmitter release and are an indicator of neural activity (Chesler, 2003; Venton et al., 481 482 2003; Takmakov et al., 2010). Therefore, care is needed to avoid confusing changes in pH and the release of neurotransmitters such as dopamine (Venton et al., 2003). In contrast to this, electrical 483 stimulation with optimal parameters triggered a release with a shorter time-course that rapidly 484 485 returned to baseline, making electrical stimulation with optimal parameters much more suitable for FSCV recordings in zebrafish. We obtained similar cyclic voltammograms by either electrically 486 stimulating the adult zebrafish telencephalon or exposing an electrode in the flow cell to dopamine 487 and histamine in the presence of an acidic pH shift (-0.5 pH units) (Fig. 4E and 6E). This acidification 488 489 fits within the normal physiological limit of pH changes (Chesler, 2003) and suggests that some of our current measurements in the adult zebrafish brain may have been influenced by alterations in pH 490 491 concomitant with neurotransmitter release. Interestingly, the low concentration of 5-HT predicted by principal component analysis (PCA) suggests that this neurotransmitter may not contribute to the in 492

vitro signal that we recorded; the trace level of 5-HT detected here could be an overestimation, caused
by the overlapping oxidation potentials of 5-HT and dopamine, or the slight shift in oxidation
potentials that can occur in tissue vs. flow cell recordings (Keithley and Wightman, 2011). Further
experiments would be required to investigate this issue.

#### 497 Validation of FSCV data

498 We used CV match and PCA (Heien et al., 2005;Keithley and Wightman, 2011) to assess how well our training set fitted the data and to separate the constituent parts of the voltammograms elicited 499 following stimulation of the telencephalon. The CV match programme calculated  $r^2$  values that 500 exceeded the statistical threshold of 0.75 in each case (Fig. 7), permitting us to conclude that it was 501 highly likely we were measuring the release of dopamine, histamine and a change of -0.25 pH units. 502 The CV match algorithm returns very conservative  $r^2$  estimates (Heien et al., 2003) meaning that we 503 can be confident in the accuracy of this result. In contrast to this, we could not produce an 504 electrochemical trace in the flow cell that surpassed the  $r^2$  threshold of 0.75 when compared to the 505 change occurring ~30 seconds after high  $K^+$  aCSF stimulation (Fig. 2F and 7F), perhaps due a 506 distortion of the signal by high K<sup>+</sup> levels and a change in pH (Threlfell and Cragg, 2007). We 507 therefore cannot conclude anything about the analytes which may contribute to this change in current. 508 509 We used PCA to partially account for our in vitro data by uploading a training set containing dopamine, 5-HT and histamine and both acidic- and basic pH changes (Fig. 8). The quality of the 510 511 PCA may be improved by using a biologically relevant training set rather than in vitro flow cell data. However, this was not achievable since initially we did not know which analytes we were detecting in 512 the zebrafish brain. Future analyses could be improved by using green fluorescent protein (GFP) 513 514 labelling to unambiguously identify neurons - for example, the ETvmat2:eGFP line labels all monoaminergic neurons in the brain (Wen et al., 2008). 515

#### 516 <u>Neurochemical profile of the zebrafish brain</u>

Stimulation of the zebrafish telencephalon appeared to trigger release of more than one 517 518 neurotransmitter. FSCV has already been used to demonstrate the simultaneous release of 5-HT and 519 histamine in the rat substantia nigra pars reticulata (Hashemi et al., 2011). Furthermore, the histamine 520 H3 heteroreceptor can modulate the activity of many types of neurons (including dopamine and 5-HT 521 neurons) thus permitting cross-talk between neurotransmitter systems (Haas et al., 2008). Zebrafish 522 dopaminergic and histaminergic neurons project extensively throughout the brain (Eriksson et al., 1998;Kaslin and Panula, 2001) making it perhaps unsurprising that histamine and dopamine could be 523 524 co-released in the telencephalon. The primary target of ascending histamine projections is the rostral medial dorsal telencephalon with some fibres innervating the caudal medial dorsal telencephalon 525 526 (Eriksson et al., 1998). Therefore, the anatomical localisation of histamine-positive fibres suggests 527 that release of histamine could contribute to the change in current that we measured. Histamine plays 528 a role in aggression, sleep, anxiety, locomotion and long-term memory in zebrafish (Peitsaro et al., 529 2000;Peitsaro et al., 2003;Renier et al., 2007;Norton et al., 2011). The absence or scarcity of this neurotransmitter in the periphery (Eriksson et al., 1998) raises the possibility that histamine may have 530 531 a more important role in the central nervous system of zebrafish than other vertebrates. Further work 532 comparing the behavioural function of histamine in fish and other model organisms will be required to 533 clarify this issue. Importantly, the protocol that we have established here can be used to examine the 534 zebrafish dopaminergic system, including comparisons of dopamine reuptake in different brain areas 535 and looking at the effect of pharmacological manipulations on neurotransmitter release. In addition, it will provide the basis for further characterisation of zebrafish mutant lines that display alterations in 536 537 behaviour. FSCV thus represents another useful tool for in-depth characterisation of the zebrafish 538 brain.

539

#### 540 <u>Author contributions</u>

541

LJ, JM, AY and WN designed the experiments. LJ conducted the experiments. WN wrote the first
version of the manuscript. LJ, JM, AY and WN improved the manuscript and approved the final
version. We have no conflicts of interest to declare.

545

#### 546 <u>Acknowledgements</u>

We are grateful to Carl Breaker for maintaining our aquarium facilities and fish care. We also thank all members of the Norton lab for helpful discussions about this data. Sandra Beleza and Jonathan McDearmid helped improve an early version of this manuscript. Vincenzo Marra, Mike Jay and Bethany Denton kindly provided help and advice during in vitro experiments and statistical analysis. Research in our laboratory is funded by the BBSRC MIBTP programme (LJJ), the European Union's seventh framework programme Aggressotype grant agreement no. 602805 and the Marie Skłodowska-Curie Foundation international training network "MiND" grant agreement no. 643051.

554

#### 555 Figure legends

#### 556 Figure 1. Fast scan cyclic voltammetry (FCSV) setup and position of the stimulating- and 557 recording electrodes.

(A) Diagram showing components of the FSCV setup and the position of the recording electrode in 558 559 the adult zebrafish brain. The applied voltage waveform (top graph) and a representative cyclic 560 voltammogram for dopamine (lower graph) are also shown, with the forward scan in black and the 561 reverse scan in red. (B) Schematic representation showing a lateral and dorsal view of the adult 562 zebrafish brain. The black asterisk marks the position of the recording electrode in the telencephalon. (C) Diagram showing characteristic non-Faradaic background signal that is subtracted to generate the 563 background-subtracted voltammograms shown throughout the paper. Abbreviations: Cb, cerebellum; 564 Hy, hypothalamus; OB, olfactory bulb; T, telencephalon; TeO, optic tectum. 565

# Figure 2. Comparison of cyclic voltammograms generated by exposing electrodes to dopamine, 5-HT, histamine and pH changes in a flow cell.

568 Colour plots (A,C,E,G,I and K) and cyclic voltammograms (B,D,F,H,J and L; black lines represent 569 forward scan and red lines reverse scan) taken at the time point indicated by the dashed white lines. 570 (A,B) 1  $\mu$ M dopamine solution. (C,D) 0.5  $\mu$ M 5-HT solution. (E,F) 40  $\mu$ M histamine solution. (G,H) 571 -0.25 units acidic pH change (pH 7.4  $\rightarrow$  pH 7.15). (I,J) -1.0 units acidic pH change (pH 7.4  $\rightarrow$  pH 572 6.4). (K,L) +1.0 units basic pH change (pH 7.4  $\rightarrow$  pH 7.4  $\rightarrow$  pH 8.4). Scale bar in A,C,E,G,I and K 573 represents 5 seconds.

#### 574 Figure 3. Comparison of analytes evoked by high K<sup>+</sup> aCSF stimulation of the zebrafish 575 telencephalon.

576 (A) Colour plot showing changes in current following stimulation with high  $K^+$  aCSF. (B) Applied waveform ranging from  $0 \text{ V} \rightarrow +1.2 \text{ V} \rightarrow -0.6 \text{ V} \rightarrow 0 \text{ V}$  (the holding potential). The forward scan of 577 the waveform is coloured black and the reverse scan is red. (C) Current vs. time plot showing the 578 579 profile of current changes at  $E_{app} = -+0.6$  V, the point in the waveform indicated by the black circle in (E). (D) Current vs. time plot showing the profile of current changes at  $E_{app} = +1.0$  V on the reverse 580 scan of the waveform, the point indicated by the circle in (F). (E) Representative cyclic 581 582 voltammogram taken at the time point indicated by the thick dashed white line in (A). (F) Representative cyclic voltammogram taken at the time point indicated by the thin dashed white line in 583 (A). (G) Cyclic voltammograms from 24 separate stimulations taken at the time point indicated by the 584 thick dashed white line in (A). (H) Cyclic voltammograms from 20 independent experiments taken at 585 586 the time point indicated by the thin dashed white line in (A). (I) Average cyclic voltammogram

derived from data presented in (G). (J) Average cyclic voltammogram derived from data presented in(H).

#### 589 Figure 4. Comparison of electrically-stimulated release of analytes in the telencephalon.

590 (A) Schematic representation showing lateral view of zebrafish telencephalon. The red crosses show 591 the position of tips of the stimulating electrode and the black cross shows the position of the recording 592 electrode used in these experiments. (B,C) Voltammograms and current vs. time plots from 8 repeated stimulations in one slice using optimal parameters (20 pulses (pulse width of 4 ms) and a voltage of 593 594 500 µA, 60 Hz). (D-F) Colour plot, voltammogram and current vs. time plot from a single 595 representative experiment using optimal stimulation. (G-I) Colour plot, voltammogram and current vs. 596 time plot from a single representative experiment using low intensity stimulation parameters (20 pulses (pulse width of 4 ms), and a voltage of 300 µA, 60 Hz). (J-L) colour plot and voltammogram 597 and current vs. time plots from a single representative experiment using high intensity stimulation 598 599 parameters (60 pulses (pulse width of 4 ms), voltage of 1 mA, 60 Hz). High intensity stimulation led 600 to the release of analytes at two different points in the voltammogram (black and red lines in L). 601 (D,G,J) Dashed lines show the position at which the voltammograms were extracted and black and red circles depict points at which current vs. time plots were taken. 602

#### 603 Figure 5. Comparison of stimulation with high K<sup>+</sup> aCSF with- and without HEPES buffer

(A) Colour plot showing changes in current evoked by stimulation with high K<sup>+</sup> aCSF without 604 HEPES. The same colour plot is shown in Fig. 2A. (B) Colour plot showing changes in current 605 evoked by stimulation with high K<sup>+</sup> aCSF containing HEPES buffer. Thick dashed white line shows 606 607 the time point and potential at which the first analyte was maximal. Thin dashed white line shows the time point at which the second analyte was observed. Current vs. time plots for responses obtained in 608 high K+ aCSF without HEPES (C) (same traces as shown in Fig. 2C and 2E for comparison) 609 compared to aCSF containing HEPES buffer (D). Blue lines show dopamine-like current and black 610 lines show histamine-like current. (E) Voltammogram extracted at time point indicated by thick 611 612 dashed white line in (B). Circle corresponds to blue line in (D). (F) Voltammogram extracted at time point indicated by thin white line in (B). Circle corresponds to black line in (D). 613

#### Figure 6. Comparison of cyclic voltammograms generated by exposing electrodes to mixtures of dopamine, 5-HT and histamine and pH changes in a flow cell.

(A) 1  $\mu$ M dopamine and 40  $\mu$ M histamine solutions. (B) 2  $\mu$ M dopamine and 20  $\mu$ M histamine 616 solutions. (C) 0.25 µM 5-HT and 40 µM histamine solutions. (D) 0.25 µM 5-HT, 1µM dopamine and 617 20 µM histamine solutions. (E) Voltammogram resulting from exposing an electrode in a flow cell to 618 619 1  $\mu$ M dopamine and 40  $\mu$ M histamine in the presence of an acidic pH shift (-0.5 pH units, pH 7.4  $\rightarrow$ pH 6.9). (F) Voltammogram resulting from exposing an electrode in a flow cell to 80 µM histamine in 620 the presence of an acidic pH shift (-0.25 pH units; pH 7.4  $\rightarrow$  pH 7.15). (G) Voltammogram resulting 621 622 from exposing an electrode in a flow cell to 1  $\mu$ M dopamine and 40  $\mu$ M histamine in the presence of a 623 basic pH shift (+1.0 pH units, pH 7.4  $\rightarrow$  pH 8.4). (H) Voltammogram resulting from exposing an 624 electrode in a flow cell to 1  $\mu$ M 5-HT and 80  $\mu$ M histamine in the presence of an acidic pH shift (-0.5 625 pH units, pH  $7.4 \rightarrow$  pH 6.9). Black lines represent forward scan and red lines reverse scan.

#### 626 Figure 7. Statistical analysis of stimulated release

627 (A) Template voltammogram resulting from exposing an electrode in a flow cell to 2  $\mu$ M dopamine 628 and 80  $\mu$ M histamine in the presence of an acidic pH shift (-0.25 pH units, pH 7.4  $\rightarrow$  pH 7.15). (B) 629 Template voltammogram resulting from exposing an electrode in a flow cell to 2  $\mu$ M dopamine and 630 20  $\mu$ M histamine. (C-F) Cyclic voltammograms obtained by either electrical- (C,E) or high K<sup>+</sup> aCSF 631 stimulation (D,F) of the telencephalon. The  $r^2$  value for (A) and (C) is 0.846; the  $r^2$  value for (A) and

## 632 (E) is 0.833; the $r^2$ value for (B) and (D) is 0.857 and the $r^2$ value for (B) and (F) is 0.416.

#### 633 Figure 8. Principal component analysis

- 634 Principal component analysis (PCA) of data obtained from stimulation of zebrafish telencephalon. (A)
- 635 Colour plot showing current changes resulting from electrical stimulation. (B) Residual colour plot
- showing changes not accounted for by the PCA model. (C) Time vs. concentration plot for dopamine
- 637 obtained from PCA. (C) Time vs. concentration plot for 5-HT obtained from PCA. (E) Time vs. 638 concentration plot for histamine obtained from PCA. (F) Time vs. pH units plot obtained from PCA.
- (G) Qt plot showing that data does not exceed the Q threshold of 686681. (H) Application of the
- model to a cyclic voltammogram representing a combination of 1  $\mu$ M dopamine, 0.25  $\mu$ M 5HT, 40
- 641  $\mu$ M histamine and a pH shift of +1.0 unit measured in a flow cell.

#### Figure 9. Dopamine reuptake inhibition with cocaine modifies analyte release profile in the telencephalon

- (A-D) Colour plots showing the time course (x-axis) of changes in current as a function of the applied 644 waveform (y-axis) after a control stimulation (A) and 10 (B), 20 (C) and 40 (D) minutes after 10 µM 645 646 cocaine administration. (E-H) Current vs. time plots showing the time course of changes in current after a control stimulation (E) and 10 (F), 20 (G) and 40 (H) minutes after 10 µM cocaine 647 administration. (I-L) Cyclic voltammograms extracted immediately following onset of release with 648 649 oxidation and reduction peaks becoming larger at  $\sim+0.65$  V and  $\sim-0.25$  V over time; control 650 stimulation (I) and 10 (J), 20 (K) and 40 (L) minutes after 10 µM cocaine administration. (M-P) Individual data points showing peak height (M), peak area (N), half width (O) and T half (P) for 651 control stimulations (C1, C2, C3) or at the time points indicated. 652
- Figure 10. Dopamine reuptake inhibition with GBR 12909 modifies analyte release profile in the telencephalon
- 655 (A-D) Colour plots showing the time course (x-axis) of changes in current as a function of the applied 656 waveform (y-axis) after a control stimulation (A) and 10 (B), 20 (C) and 40 (D) minutes after 10 µM GBR 12909 administration. (E-H) Current vs. time plots showing the time course of changes in 657 current after a control stimulation (E) and 10 (F), 20 (G) and 40 (H) minutes after 10 µM GBR 12909 658 administration. (I-L) Cyclic voltammograms extracted immediately following onset of release, with 659 660 oxidation and reduction peaks becoming larger at ~+0.65 V and ~-0.25 V over time; control stimulation (I) and 10 (J), 20 (K) and 40 (L) minutes after 10 µM GBR 12909 administration. Current 661 662 vs. time plots showing the time course of changes in current after a control stimulation (I) and 10 (J), 20 (K) and 40 (L) minutes after 10 µM GBR 12909 administration. (M-P) Individual data points 663 showing peak height (M), peak area (N), half width (O) and T half (P) for control stimulations (C1, 664 C2, C3) or at the time points indicated. 665
- 666

667

#### 668 <u>References</u>

- Arrenberg, A.B., and Driever, W. (2013). Integrating anatomy and function for zebrafish circuit
  analysis. *Frontiers in Neural Circuits* 7, 74. doi: 10.3389/fncir.2013.00074.
- Bargmann, C.I. (2012). Beyond the connectome: How neuromodulators shape neural circuits.
   *BioEssays* 34, 458-465. doi: 10.1002/bies.201100185.
- Baur, J.E., Kristensen, E.W., May, L.J., Wiedemann, D.J., and Wightman, R.M. (1988). Fast-scan
  voltammetry of biogenic amines. *Analytical Chemistry* 60, 1268-1272. doi:
  10.1021/ac00164a006.
- Bonan, C.D., and Norton, W.H.J. (2015). The utility of zebrafish as a model for behavioural genetics.
   *Current Opinion in Behavioral Sciences* 2, 34-38. doi: http://dx.doi.org/10.1016/j.cobeha.2014.07.003.
- Buske, C., and Gerlai, R. (2012). Maturation of shoaling behavior is accompanied by changes in the
  dopaminergic and serotoninergic systems in zebrafish. *Developmental Psychobiology* 54, 2835. doi: 10.1002/dev.20571.

- Chang, S.-Y., Jay, T., Muñoz, J., Kim, I., and Lee, K.H. (2012). Wireless fast-scan cyclic
   voltammetry measurement of histamine using WINCS -- a proof-of-principle study. *The Analyst* 137, 2158-2165. doi: 10.1039/c2an16038b.
- 685 Chesler, M. (2003). Regulation and Modulation of pH in the Brain. *Physiol Rev.* 83, 1183-1221. doi: 10.1152/physrev.00010.2003.
- 687 Curado, S., Anderson, R.M., Jungblut, B., Mumm, J., Schroeter, E., and Stainier, D.Y.R. (2007).
  688 Conditional targeted cell ablation in zebrafish: A new tool for regeneration studies.
  689 Developmental Dynamics 236, 1025-1035. doi: 10.1002/dvdy.21100.
- Dankoski, E.C., and Wightman, R.M. (2013). Monitoring serotonin signaling on a subsecond time
   scale. *Frontiers in integrative neuroscience* 7, 44. doi: 10.3389/fnint.2013.00044.
- Davidson, R.J., Putnam, K.M., and Larson, C.L. (2000). Dysfunction in the neural circuitry of
   emotion regulation A possible prelude to violence. *Science* 289, 591-594.
- Del Bene, F., and Wyart, C. (2012). Optogenetics: A new enlightenment age for zebrafish
   neurobiology. *Developmental Neurobiology* 72, 404-414. doi: 10.1002/dneu.20914.
- Eriksson, K.S., Peitsaro, N., Karlstedt, K., Kaslin, J., and Panula, P. (1998). Development of the
  histaminergic neurons and expression of histidine decarboxylase mRNA in the zebrafish brain
  in the absence of all peripheral histaminergic systems. *European Journal of Neuroscience* 10,
  3799-3812. doi: 10.1046/j.1460-9568.1998.00394.x.
- España, R.A., Roberts, D.C.S., and Jones, S.R. (2008). Short-acting cocaine and long-acting GBR 12909 both elicit rapid dopamine uptake inhibition following intravenous delivery.
   *Neuroscience* 155, 250-257. doi: 10.1016/j.neuroscience.2008.05.022.
- Esposti, F., Johnston, J., Rosa, Juliana m., Leung, K.-M., and Lagnado, L. (2013). Olfactory
  Stimulation Selectively Modulates the OFF Pathway in the Retina of Zebrafish. *Neuron* 79, 97-110. doi: 10.1016/j.neuron.2013.05.001.
- Feierstein, C.E., Portugues, R., and Orger, M.B. Seeing the whole picture: A comprehensive imaging
   approach to functional mapping of circuits in behaving zebrafish. *Neuroscience* [Online].
   Available: <u>http://www.sciencedirect.com/science/article/pii/S0306452214010148</u>.
- Fetcho, J.R., and Liu, K.S. (1998). Zebrafish as a Model System for Studying Neuronal Circuits and
  Behaviora. *Annals of the New York Academy of Sciences* 860, 333-345. doi: 10.1111/j.17496632.1998.tb09060.x.
- Fortin, S.M., Cone, J.J., Ng-Evans, S., Mccutcheon, J.E., and Roitman, M.F. (2015). Sampling phasic
   dopamine signaling with fast-scan cyclic voltammetry in awake, behaving rats. *Curr Protoc Neurosci* 70, 7.25.21-27.25.20. doi: 10.1002/0471142301.ns0725s70.
- Haas, H.L., Sergeeva, O.A., and Selbach, O. (2008). Histamine in the Nervous System. *Physiological Reviews* 88, 1183-1241. doi: 10.1152/physrev.00043.2007.
- Hashemi, P., Dankoski, E.C., Wood, K.M., Ambrose, R.E., and Wightman, R.M. (2011). In vivo
  electrochemical evidence for simultaneous 5-HT and histamine release in the rat substantia
  nigra pars reticulata following medial forebrain bundle stimulation. *Journal of Neurochemistry* 118, 749-759. doi: 10.1111/j.1471-4159.2011.07352.x.
- Heien, M.L., Phillips, P.E., Stuber, G.D., Seipel, A.T., and Wightman, R.M. (2003). Overoxidation of
   carbon-fiber microelectrodes enhances dopamine adsorption and increases sensitivity. *Analyst* 128, 1413-1419. doi: 10.1039/b307024g.
- Heien, M.L.a.V., Johnson, M.A., and Wightman, R.M. (2004). Resolving Neurotransmitters Detected
   by Fast-Scan Cyclic Voltammetry. *Analytical Chemistry* 76, 5697-5704. doi:
   10.1021/ac0491509.
- Heien, M.L.a.V., Khan, A.S., Ariansen, J.L., Cheer, J.F., Phillips, P.E.M., Wassum, K.M., and
  Wightman, R.M. (2005). Real-time measurement of dopamine fluctuations after cocaine in
  the brain of behaving rats. *Proceedings of the National Academy of Sciences of the United States of America* 102, 10023-10028. doi: 10.1073/pnas.0504657102.
- Higashijima, S.-I., Masino, M.A., Mandel, G., and Fetcho, J.R. (2003). Imaging Neuronal Activity
   During Zebrafish Behavior With a Genetically Encoded Calcium Indicator. *Journal of Neurophysiology* 90, 3986-3997. doi: 10.1152/jn.00576.2003.
- John, C.E., and Jones, S.R. (2007a). "Fast Scan Cyclic Voltammetry of Dopamine and Serotonin in
   Mouse Brain Slices," in *Electrochemical Methods for Neuroscience*, eds. A.C. Michael &
   L.M. Borland. (Boca Raton (FL): CRC Press).

- John, C.E., and Jones, S.R. (2007b). Voltammetric characterization of the effect of monoamine uptake
   inhibitors and releasers on dopamine and serotonin uptake in mouse caudate-putamen and
   substantia nigra slices. *Neuropharmacology* 52, 1596-1605.
- Jones, S.R., Garris, P.A., Kilts, C.D., and Wightman, R.M. (1995a). Comparison of Dopamine Uptake
  in the Basolateral Amygdaloid Nucleus, Caudate-Putamen, and Nucleus Accumbens of the
  Rat. *Journal of Neurochemistry* 64, 2581-2589. doi: 10.1046/j.1471-4159.1995.64062581.x.
- Jones, S.R., Garris, P.A., and Wightman, R.M. (1995b). Different effects of cocaine and nomifensine
   on dopamine uptake in the caudate-putamen and nucleus accumbens. *Journal of Pharmacology and Experimental Therapeutics* 274, 396-403.
- Jones, S.R., Mickelson, G.E., Collins, L.B., Kawagoe, K.T., and Mark Wightman, R. (1994).
  Interference by pH and Ca2+ ions during measurements of catecholamine release in slices of rat amygdala with fast-scan cyclic voltammetry. *Journal of Neuroscience Methods* 52, 1-10.
  doi: http://dx.doi.org/10.1016/0165-0270(94)90048-5.
- Kaslin, J., and Panula, P. (2001). Comparative anatomy of the histaminergic and other aminergic
  systems in zebrafish (Danio rerio). *The Journal of Comparative Neurology* 440, 342-377. doi:
  10.1002/cne.1390.
- Keithley, R.B., and Wightman, R.M. (2011). Assessing Principal Component Regression Prediction
   of Neurochemicals Detected with Fast-Scan Cyclic Voltammetry. *ACS Chemical Neuroscience* 2, 514-525. doi: 10.1021/cn200035u.
- Lillesaar, C., Stigloher, C., Tannhäuser, B., Wullimann, M.F., and Bally-Cuif, L. (2009). Axonal
   projections originating from raphe serotonergic neurons in the developing and adult zebrafish,
   Danio rerio, using transgenics to visualize raphe-specific pet1 expression. *The Journal of Comparative Neurology* 512, 158-182. doi: 10.1002/cne.21887.
- Nagel, G., Szellas, T., Huhn, W., Kateriya, S., Adeishvili, N., Berthold, P., Ollig, D., Hegemann, P.,
  and Bamberg, E. (2003). Channelrhodopsin-2, a directly light-gated cation-selective
  membrane channel. *Proceedings of the National Academy of Sciences of the United States of America* 100, 13940-13945. doi: 10.1073/pnas.1936192100.
- Naumann, E.A., Kampff, A.R., Prober, D.A., Schier, A.F., and Engert, F. (2010). Monitoring neural activity with bioluminescence during natural behavior. *Nat Neurosci* 13, 513-520. doi:
   <u>http://www.nature.com/neuro/journal/v13/n4/suppinfo/nn.2518\_S1.html</u>.
- Near, J.A., Bigelow, J.C., and Wightman, R.M. (1988). Comparison of uptake of dopamine in rat
   striatal chopped tissue and synaptosomes. *Journal of Pharmacology and Experimental Therapeutics* 245, 921-927.
- Norton, W.H.J., Stumpenhorst, K., Faus-Kessler, T., Folchert, A., Rohner, N., Harris, M.P., Callebert,
  J., and Bally-Cuif, L. (2011). Modulation of Fgfr1a Signaling in Zebrafish Reveals a Genetic
  Basis for the Aggression–Boldness Syndrome. *The Journal of Neuroscience* 31, 1379613807. doi: 10.1523/jneurosci.2892-11.2011.
- Peitsaro, N., Anichtchik, O.V., and Panula, P. (2000). Identification of a Histamine H3-like Receptor
  in the Zebrafish (Danio rerio) Brain. *Journal of Neurochemistry* 75, 718-724. doi:
  10.1046/j.1471-4159.2000.0750718.x.
- Peitsaro, N., Kaslin, J., Anichtchik, O.V., and Panula, P. (2003). Modulation of the histaminergic
  system and behaviour by α-fluoromethylhistidine in zebrafish. *Journal of Neurochemistry* 86,
  432-441. doi: 10.1046/j.1471-4159.2003.01850.x.
- Pihel, K., Hsieh, S., Jorgenson, J.W., and Wightman, R.M. (1995). Electrochemical detection of
  histamine and 5-hydroxytryptamine at isolated mast cells. *Analytical Chemistry* 67, 45144521. doi: 10.1021/ac00120a014.
- Renier, C., Faraco, J.H., Bourgin, P., Motley, T., Bonaventure, P., Rosa, F., and Mignot, E. (2007).
  Genomic and functional conservation of sedative-hypnotic targets in the zebrafish. *Pharmacogenet Genomics* 17, 237-253. doi: 10.1097/FPC.0b013e3280119d62.
- Robinson, D.L., Venton, B.J., Heien, M.L., and Wightman, R.M. (2003). Detecting subsecond
   dopamine release with fast-scan cyclic voltammetry in vivo. *Clin Chem* 49, 1763-1773.
- Robinson, D.L., and Wightman, R.M. (2007). "Rapid Dopamine Release in Freely Moving Rats.," in
   *Electrochemical Methods for Neuroscience.*, eds. Michael A.C. & B. L.M. (Boca Raton (FL):
   CRC Press).

- Sinkala, E., Mccutcheon, J.E., Schuck, M., Schmidt, E., Roitman, M.F., and Eddington, D.T. (2012).
   Electrode Calibration with a Microfluidic Flow Cell for Fast-scan Cyclic Voltammetry. *Lab on a chip* 12, 2403-2408. doi: 10.1039/c2lc40168a.
- Stamford, J.A. (1990). Fast cyclic voltammetry: Measuring transmitter release in 'real time'. *Journal* of Neuroscience Methods 34, 67-72. doi: <u>http://dx.doi.org/10.1016/0165-0270(90)90043-F</u>.
- Takmakov, P., Zachek, M.K., Keithley, R.B., Bucher, E.S., Mccarty, G.S., and Wightman, R.M.
  (2010). Characterization of Local pH Changes in Brain Using Fast-Scan Cyclic Voltammetry
  with Carbon Microelectrodes. *Analytical Chemistry* 82, 9892-9900. doi: 10.1021/ac102399n.
- Threlfell, S., and Cragg, S.J. (2007). "Using Fast-Scan Cyclic Voltammetry to Investigate
  Somatodendritic Dopamine Release," in *Electrochemical Methods for Neuroscience*, eds.
  A.C. Michael & L.M. Borland. (Boca Raton (FL): CRC Press
- 802 Taylor & Francis Group, LLC).
- Vargas, R., Jóhannesdóttir, I.Þ., Sigurgeirsson, B., Þorsteinsson, H., and Karlsson, K.Æ. (2011). The
  zebrafish brain in research and teaching: a simple in vivo and in vitro model for the study of
  spontaneous neural activity. *Adv Physiol Educ* 35, 188-196. doi: 10.1152/advan.00099.2010.
- Venton, B.J., Michael, D.J., and Wightman, R.M. (2003). Correlation of local changes in extracellular
   oxygen and pH that accompany dopaminergic terminal activity in the rat caudate–putamen.
   *Journal of Neurochemistry* 84, 373-381. doi: 10.1046/j.1471-4159.2003.01527.x.
- Webb, K.J., Norton, W.H.J., Trümbach, D., Meijer, A.H., Ninkovic, J., Topp, S., Heck, D., Marr, C.,
  Wurst, W., Theis, F.J., Spaink, H.P., and Bally-Cuif, L. (2009). Zebrafish reward mutants
  reveal novel transcripts mediating the behavioral effects of amphetamine. *Genome Biology*10, R81-R81. doi: 10.1186/gb-2009-10-7-r81.
- Wen, L., Wei, W., Gu, W., Huang, P., Ren, X., Zhang, Z., Zhu, Z., Lin, S., and Zhang, B. (2008).
  Visualization of monoaminergic neurons and neurotoxicity of MPTP in live transgenic
  zebrafish. *Developmental Biology* 314, 84-92. doi: http://dx.doi.org/10.1016/j.ydbio.2007.11.012.
- Westerfield, M. (1995). *The Zebrafish Book. A Guide for the Laboratory Use of Zebrafish (Danio rerio), 3rd Edition.* Eugene, OR: University of Oregon Press.
- Yorgason, J.T., España, R.A., and Jones, S.R. (2011). Demon voltammetry and analysis software:
  Analysis of cocaine-induced alterations in dopamine signaling using multiple kinetic
  measures. *Journal of neuroscience methods* 202, 158-164. doi:
  10.1016/j.jneumeth.2011.03.001.
- Zhang, F., Wang, L.-P., Brauner, M., Liewald, J.F., Kay, K., Watzke, N., Wood, P.G., Bamberg, E.,
   Nagel, G., Gottschalk, A., and Deisseroth, K. (2007). Multimodal fast optical interrogation of
   neural circuitry. *Nature* 446, 633-639. doi:
- 826 <u>http://www.nature.com/nature/journal/v446/n7136/suppinfo/nature05744\_S1.html</u>.
- Ziv, L., Muto, A., Schoonheim, P.J., Meijsing, S.H., Strasser, D., Ingraham, H.A., Schaaf, M.J.M.,
   Yamamoto, K.R., and Baier, H. (2013). An affective disorder in zebrafish with mutation of
   the glucocorticoid receptor. *Molecular psychiatry* 18, 681-691. doi: 10.1038/mp.2012.64.
- Zupanc, G.K.H., and Lamprecht, J. (2000). Towards a Cellular Understanding of Motivation:
   Structural Reorganization and Biochemical Switching as Key Mechanisms of Behavioral
   Description: Defendence of the state of
- 832
   Plasticity. *Ethology* 106, 467-477. doi: 10.1046/j.1439-0310.2000.00546.x.
- 833

834

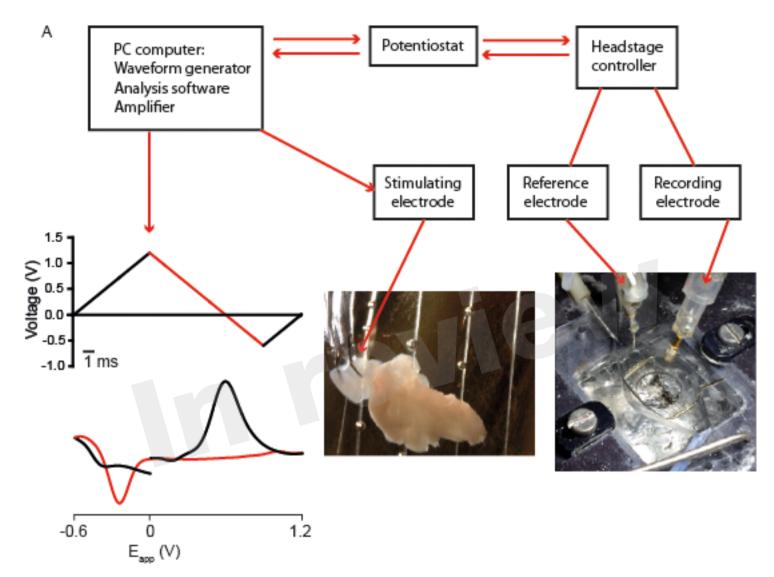
#### 835 Table 1

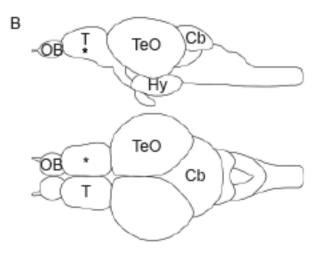
- 836 Output for CV Match linear regression analysis comparing template cyclic voltammograms obtained
- using a flow cell with cyclic voltammograms extracted from experimental data obtained using either
- 838 optimal electrical stimulation parameters (n=4 stimulations from 2 sagittal sections taken from 2 fish)
- 839 or K+ stimulation (n=2 stimulations from 2 fish). Bold type indicates a significant  $r^2$  value, and bold
- red type indicates the highest  $r^2$  value for the example stimulation. Legend: DA, dopamine; HA,
- 841 histamine; Estim, electrical stimulation;  $K^+$ , high  $K^+$  aCSF stimulation.

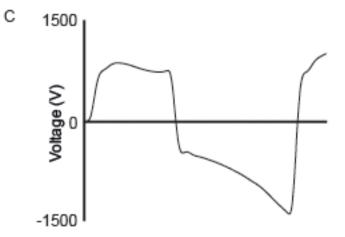
DA (μM)	HA (µM)	5-ΗΤ (μM)	Acid pH (pH units)	Basic pH (pH units)	ESti m1 ( <i>r</i> <sup>2</sup> )	Esti m2 (r <sup>2</sup> )	Esti m3 (r <sup>2</sup> )	Esti m4 (r <sup>2</sup> )	K <sup>+</sup> 10s 1 (r <sup>2</sup> )	K <sup>+</sup> 30s 1 (r <sup>2</sup> )	K <sup>+</sup> 10s 2 (r <sup>2</sup> )	K <sup>+</sup> 30s 2 (r <sup>2</sup> )
0.5	0	0	0	0	0.053	0.213	0.321	0.121	0.551	0.123	0.542	0.081
1	0	0	0	0	0.639	0.657	0.602	0.638	0.78	0.316	0.836	0.408
2	0	0	0	0	0.61	0.624	0.56	0.512	0.742	0.325	0.81	0.369
0	10	0	0	0	0.167	0.164	0.366	0.377	0.75	0.373	0.465	0.361
0	20	0	0	0	0.061	0.2	0.155	0.222	0.691	0.306	0.417	0.313
0	40	0	0	0	0.199	0.284	0.053	0.179	0.702	0.468	0.559	0.52
0	0	0.1	0	0	0.661	0.678	0.641	0.73	0.758	0.414	0.74	0.612
0	0	0.5	0	0	0.625	0.611	0.671	0.664	0.694	0.375	0.659	0.402
0	0	0.25	0	0	0.529	0.456	0.474	0.493	0.548	0.319	0.482	0.248
0	0	0	0	0.5	0.468	0.436	0.703	0.679	0.478	0.197	0.418	0.139
0	0	0	0	1	0.669	0.579	0.814	0.843	0.353	0.154	0.55	0.211
0	0	0	0	2	0.599	0.604	0.834	0.871	0.235	0.288	0.533	0.205
0	0	0	0.5	0	0.348	0.254	0.641	0.652	0.633	0.139	0.198	0.071
0	0	0	0.25	0	0.368	0.297	0.624	0.688	0.556	0.166	0.245	0.045
0	0	0	1	0	0.291	0.311	0.59	0.588	0.624	0.194	0.275	0.145
0	0	0	3.5	0	0.385	0.485	0.576	0.509	0.465	0.51	0.528	0.432
1	40	0	0	0	0.561	0.611	0.352	0.47	0.833	0.45	0.76	0.524
2	20	0	0	0	0.814	0.787	0.771	0.651	0.857	0.416	0.866	0.441
0	40	0.25	0	0	0.71	0.67	0.588	0.65	0.762	0.425	0.674	0.463
1	20	0.25	0	0	0.776	0.746	0.784	0.733	0.853	0.426	0.814	0.431
1	0	0	0	0.5	0.31	0.101	0.379	0.399	0.475	0.374	0.267	0.011
4	0	0	0	1	0.427	0.328	0.209	0.202	0.327	0.508	0.508	0.337
2	0	0	0.5	0	0.833	0.755	0.832	0.868	0.734	0.282	0.752	0.285
4	0	0	0.25	0	0.841	0.802	0.818	0.873	0.781	0.318	0.819	0.341
1	0	0	1	0	0.667	0.588	0.724	0.801	0.588	0.19	0.626	0.151
0	40	0	0	0.5	0.19	0.254	0.402	0.48	0.651	0.24	0.325	0.216
0	40	0	0	2	0.403	0.447	0.641	0.725	0.426	0.169	0.344	0.317
0	160	0	0.5	0	0.59	0.466	0.676	0.678	0.37	0.273	0.487	0.252
0	160	0	0.25	0	0.473	0.511	0.581	0.593	0.228	0.14	0.504	0.376
0	40	0	1	0	0.548	0.435	0.705	0.713	0.245	0.148	0.454	0.092
0	0	1	0	1	0.552	0.519	0.541	0.581	0.61	0.314	0.549	0.258
0	0	0.5	0	2	0.514	0.504	0.742	0.746	0.208	0.27	0.42	0.224
0	0	0.5	2	0	0.385	0.419	0.566	0.645	0.426	0.191	0.423	0.126
2	80	0	0	0.5	0.54	0.523	0.272	0.372	0.759	0.442	0.658	0.53

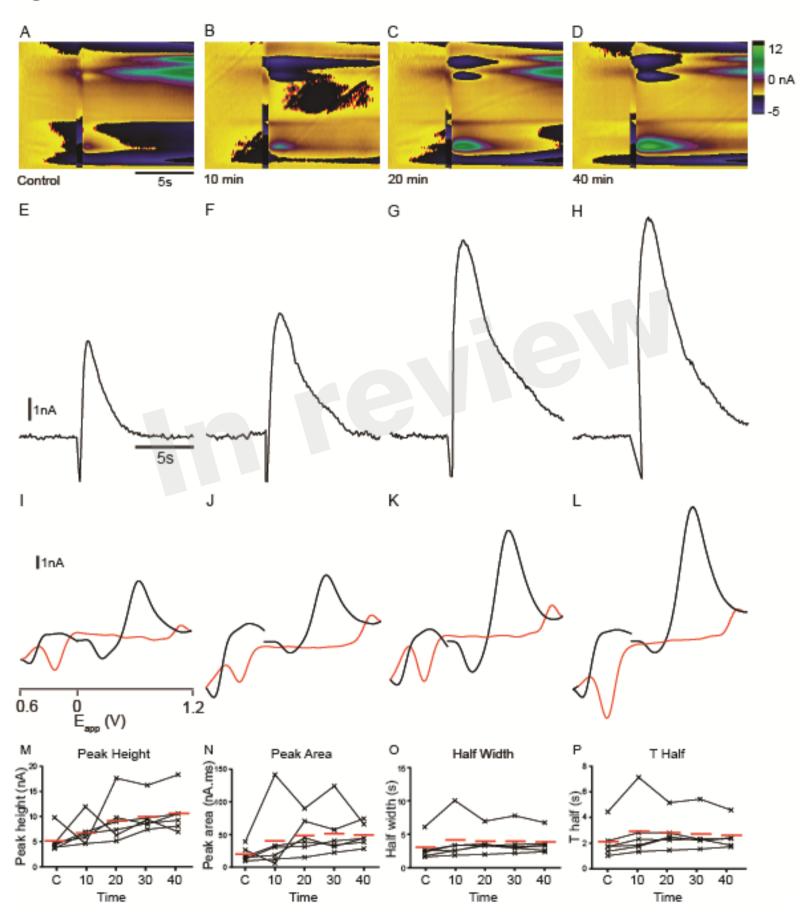
1	40	0	0	1	0.312	0.206	0.427	0.488	0.552	0.156	0.241	0.078
1	40	0	0.5	0	0.795	0.755	0.75	0.804	0.826	0.435	0.808	0.483
2	160	0	0.5	0	0.845	0.739	0.84	0.853	0.675	0.414	0.75	0.355
2	80	0	0.25	0	0.846	0.833	0.863	0.877	0.777	0.421	0.824	0.426
4	160	0	0.25	0	0.845	0.806	0.863	0.878	0.752	0.441	0.801	0.421
1	80	0	1	0	0.752	0.676	0.799	0.831	0.178	0.248	0.702	0.243
0	160	1	0.5	0	0.75	0.727	0.836	0.813	0.762	0.481	0.712	0.461
1	40	0.5	0	1	0.197	0.05	0.315	0.361	0.609	0.25	0.251	0.062

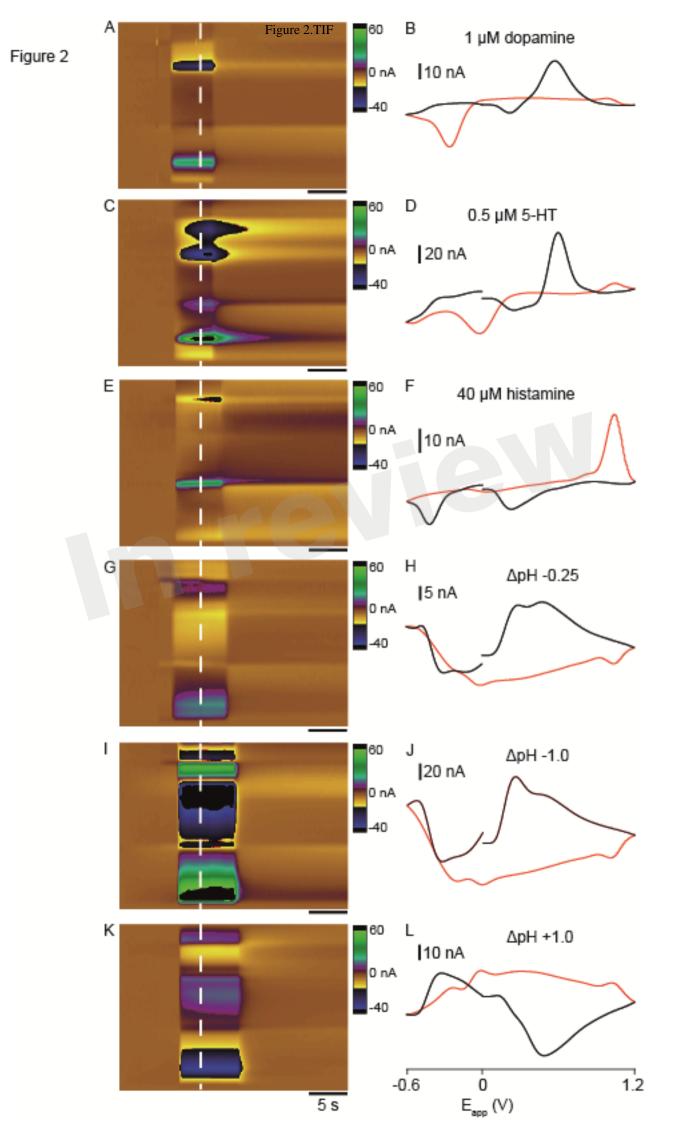














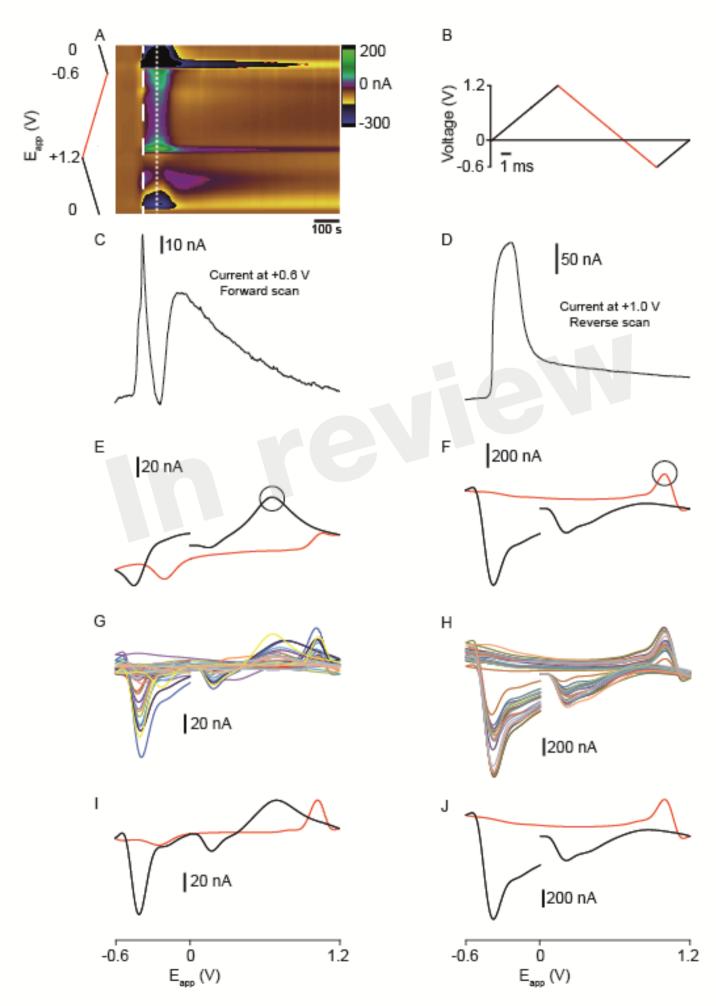


Figure 4

